Pareto Optimal Analog Beamforming Design for Integrated MIMO Radar and Communication

Pan Cao, *Member, IEEE*

***Abstract*—This work considers an integrated multi-input-multi-output (MIMO) radar and communication system, where the radar sensing and communication share the common antenna array and spectrum. A performance conflict exists between the radar sensing and communication. To explore all their performance trade-offs, it is aimed to determine the achievable signal-to-interference plus noise (SINR) region of radar sensing and communication. We formulate a Pareto optimization problem with respect to two analog beamforming vectors for radar sensing and communication, respectively - to maximize one SINR and keep the other as constant, which is cast as a rank-one constrained optimization problem. A locally optimal solution is attained by using a sequential rank-one relaxation algorithm. Simulation results illustrate the achievable SINR region and compare the performance for a case study.**

***Index Terms*—Integrated MIMO radar and communication, Pareto optimality, analog beamforming, clutter interference, rank-one optimization.**

I. Introduction

Radar and wireless communications are two most common civil and military applications via radio frequency (RF) signalling for decades, and both utilize similar hardware structure and system components in baseband and RF ends. This provides a feasible opportunity to integrate radar and communication so as to fully exploit the system potentials through sharing the hardware and RF spectrum. The challenges arising in the integrated system have attracted extensive research attention and efforts recently, e.g., some overview work in integrated sensing and communication [1]–[7], integrated localization and communication [7], [8], and integrated imaging and communication [9].

Multiple-input-multiple-output (MIMO) radar typically employs a phased antenna array with a single RF chain to generate directional analog beam(s) that points to the sensing direction of interest. For the multi-antenna communication system, e.g., massive MIMO, it is practically preferred to serve a large antenna array by using a greatly smaller number of RF chains in order to reduce the hardware complexity, energy consumption and cost. Therefore, this work studies an integrated dual-function MIMO radar and communication system (ISAC) as shown in Fig. 1, which, without loss of generality, is equipped with an N-element uniform linear array (ULA) with half-wavelength adjacent antenna spacing. The ULA response vector is expressed by

$$\boldsymbol{a}(\theta) = [1, e^{j\pi\cos(\theta)}, \ldots, e^{j\pi(N-1)\cos(\theta)}], \tag{1}$$

The author is with the School of Physics, Engineering and Computer Science, The University of Hertfordshire, Hertfordshire AL10 9AB, United Kingdom (corresponding email: p.cao@herts.ac.uk).

where $\theta \in [0, \pi]$ denotes the angle of departure (AoD) of the forward signalling or the angle of arrival (AoA) of the echoes. This N-element ULA is jointly fed by two separate RF chains - one is for communication and the other is for radar sensing. This allows the integrated system to realize dual-function of radar sensing and communication simultaneously and independently through their own RF chains but sharing the common spectrum and antenna array.

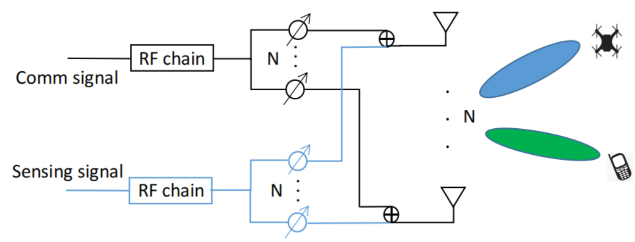

Fig. 1: Integrated MIMO radar and communication system

We define the beamforming vectors for communication and the radar sensing as $\boldsymbol{w}_c \in \mathbb{C}^{N\times 1}$ and $\boldsymbol{w}_s \in \mathbb{C}^{N\times 1}$, respectively, and both satisfy the following conditions

$$\boldsymbol{w}_s, \boldsymbol{w}_c \in \mathcal{W}, \text{ for } \mathcal{W} := \{\boldsymbol{x} \mid |\boldsymbol{x}(1)| = \ldots = |\boldsymbol{x}(N)|\} \tag{2a}$$
$$||\boldsymbol{w}_c||^2 + ||\boldsymbol{w}_s||^2 \leq P_{\max}, \tag{2b}$$

where $\boldsymbol{w}_c$ and $\boldsymbol{w}_s$ are with constant modulus and subject to a sum power constraint (2b), where $P_{\max}$ is the maximum total transmit power budget of the ISAC system. Therefore, there exists an inherent utility conflict between the radar sensing and communication based on the limited sharing resource. In this work, *the fundamental question we want to address is how we should choose the beamforming vectors $\boldsymbol{w}_c$ and $\boldsymbol{w}_s$ to balance the joint sensing and communication performance.*

To explore all the potentials of the ISAC, the two/multi-criteria achievable performance region can be used to illustrate all the achievable trade-offs. The outer boundary of the region is called Pareto boundary, because it consists of Pareto optimal operating points. A Pareto optimal point is an operating point at which one cannot improve one performance without simultaneously decreasing the other [10]. The Pareto optimization principle is useful for the beamforming design to illustrate the two/multi-user achievable rate region in multi-antenna interference channel [11]–[13]. However, there is little work on Pareto optimal joint beamforming design for the ISAC system. To our best knowledge, the only one is to study the waveform design for the dual-function integrated MIMO radar and communication [14], where the achievable performance region is formed by the multi-communication users' signl-to-interference-plus-noise ratio (SINR) and the peak sidelobe level of the sensing beam pattern for a single target with the given angle. The transmit covariance matrices (waveform) are optimized by using the weighted fairness maximization (fairness-profile) method.

In this work, we desire to achieve the Pareto optimal region of joint sensing and communication SINR by optimizing two analog beamforming vectors $\boldsymbol{w}_c$ and $\boldsymbol{w}_s$ for the ISAC system defined in Fig.1. We propose an MIMO channel model and estimation scheme in Section II, which can be used to model the clutter interference that limits the sensing SINR. In Section III, to determine each boundary operating point, we formulate a Pareto optimization problem - maximize one SINR while the other is fixed, which is cast as a non-convex rank-one optimization problem. We propose a novel sequential rank-one constraint relaxation (SROCR)-based algorithm to achieve locally optimal solutions, leading to a reasonable inner boundary of the Pareto boundary, which is numerically illustrated and compared in Section IV.

II. MIMO Radar Channel and Clutter Interference

The typical radar sensing performance is usually limited by the clutter interference that pollutes the desired targets' reflected echoes, especially for the near-ground ISAC system. The clutter interference might be severe due to the multipath reflection by the static objectives (e.g., ground, buildings, trees), which is usually much stronger than the system noise power floor, and even comparable or stronger than the desired signal returned by the targets. Therefore, there is a significant need to suppress clutter interference for the ISAC system to achieve reasonable detection performance.

For an on/near-ground stationary monostatic MIMO radar, we propose to split the two-way wireless sensing channel into two components - *target channel* reflected by the target and *clutter channel* reflected by the clutter scatters. Therefore, the MIMO radar channel can be denoted as

$$\boldsymbol{H}_s = \boldsymbol{H}_{s,t} + \boldsymbol{H}_{s,c}, \tag{3}$$

where $\boldsymbol{H}_{s,t}, \boldsymbol{H}_{s,c} \in \mathbb{C}^{N\times N}$ denote target channel and clutter sensing channel, respectively. The clutter interference can be completely cancelled by making sure $\boldsymbol{w}_s^H \boldsymbol{H}_{s,c} \boldsymbol{w}_s = 0$, i.e., $\boldsymbol{w}_s$ should be in the null space of $\boldsymbol{H}_{s,c}$. Instead, the soft control of the clutter interference $\boldsymbol{w}_s^H \boldsymbol{H}_{s,c} \boldsymbol{w}_s$ is more applicable, especially in the rich clutter environment, which be realized by satisfying a minimum sensing SINR requirement.

We propose a two-step method to estimate the radar sensing channel as follows:

Step 1. Estimation of clutter channel $\boldsymbol{H}_{s,c}$: The MIMO sensing channel $\boldsymbol{H}_s$ becomes $\boldsymbol{H}_{s,c}$ when the target is absent. Therefore, the clutter channel $\boldsymbol{H}_{s,c}$ can be estimation in advance (when the target is absent), for example, by transmitting pilot sequences and estimating the clutter channel based on returned pilots using the linear minimum mean square error (MMSE) estimator.

Step 2. Estimation of target channel $\boldsymbol{H}_{s,t}$: The two-way target channel can be constructed as $\boldsymbol{H}_{s,t} := \alpha_t \boldsymbol{a}(\theta_t)\boldsymbol{a}^H(\theta_t)$, where the target angle θ_t and target range gain α_t can be roughly estimated during the radar periodic beam scanning procedure (i.e.,exhaustive beam swapping to detect target).

III. Pareto Optimal Beamforming Design

From the perspective of communication function, it is aimed to maximize the communication SINR for a single-antenna communication receiver, which can be formulated as the following communication SINR maximization problem:

$$\max_{\boldsymbol{w}_s,\boldsymbol{w}_c} \quad \frac{|\boldsymbol{w}_c^H \boldsymbol{h}_c|^2}{|\boldsymbol{w}_s^H \boldsymbol{h}_c|^2 + \sigma_c^2} \tag{4a}$$
$$\text{s.t.} \quad \|\boldsymbol{w}_c\|^2 + \|\boldsymbol{w}_s\|^2 \le P_{\max} \tag{4b}$$
$$\boldsymbol{w}_s, \boldsymbol{w}_c \in \mathcal{W}, \tag{4c}$$

where $\boldsymbol{h}_c \in \mathbb{C}^{N\times 1}$ denotes the communication channel. The objective function (4a) is the communication SINR, denoted by $\mathrm{SINR}_c(\boldsymbol{w}_s, \boldsymbol{w}_c)$, which is limited by the radar sensing interference. The constraint (4c) denotes the constant-modules constraint of both $\boldsymbol{w}_c$ and $\boldsymbol{w}_s$.

For the radar sensing function, it is desired to design the beamforming to observe the target of interest and meanwhile to suppress the interference, which can be formulated as the following radar sensing SINR maximization problem:

$$\max_{\boldsymbol{w}_c,\boldsymbol{w}_s} \quad \frac{\boldsymbol{w}_s^H \boldsymbol{H}_{s,t} \boldsymbol{w}_s}{(\boldsymbol{w}_s+\boldsymbol{w}_c)^H \boldsymbol{H}_{s,c}(\boldsymbol{w}_s+\boldsymbol{w}_c) + \boldsymbol{w}_c^H \boldsymbol{H}_{s,t} \boldsymbol{w}_c + \sigma_s^2} \tag{5a}$$
$$\text{s.t.} \quad \|\boldsymbol{w}_c\|^2 + \|\boldsymbol{w}_s\|^2 \le P_{\max} \tag{5b}$$
$$\boldsymbol{w}_s, \boldsymbol{w}_c \in \mathcal{W} \tag{5c}$$

where the radar sensing SINR (5a) is denoted by $\mathrm{SINR}_s(\boldsymbol{w}_s, \boldsymbol{w}_c)$ that limited by both the clutter interference and communication signalling interference.

The achievable ISAC SINR region is defined as a set of the achievable SINR pairs with all the feasible beamforming vectors $\{\boldsymbol{w}_s, \boldsymbol{w}_c\}$, i.e.,

$$\mathcal{R} := \cup_{\boldsymbol{w}_s,\boldsymbol{w}_c} (\mathrm{SINR}_c(\boldsymbol{w}_s, \boldsymbol{w}_c), \mathrm{SINR}_s(\boldsymbol{w}_s, \boldsymbol{w}_c)). \tag{6}$$

The outermost boundary of the achievable ISAC SINR region $\mathcal{R}$ is called Pareto boundary, which is denoted by a set $\mathcal{R}^\star := \cup(\mathrm{SINR}_c^\star, \mathrm{SINR}_s^\star)$ where $(\mathrm{SINR}_c^\star, \mathrm{SINR}_s^\star)$ is a Pareto-optimal point corresponding a best trade-off pair of $(\mathrm{SINR}_c(\boldsymbol{w}_s, \boldsymbol{w}_c), \mathrm{SINR}_s(\boldsymbol{w}_s, \boldsymbol{w}_c))$. At a strictly Pareto-optimal point, it is impossible to improve one performance without decreasing the other.

To achieve a Pareto-optimal point, we formulate a Pareto optimization problem that maximizes one SINR and meanwhile fixes the other. This allows the target SINR to increase gradually following a straight line until it reaches the Pareto boundary. That is,

$$\max_{\boldsymbol{w}_s,\boldsymbol{w}_c} \quad \mathrm{SINR}_c(\boldsymbol{w}_s, \boldsymbol{w}_c) \tag{7a}$$
$$\text{s.t.} \quad \mathrm{SINR}_s(\boldsymbol{w}_s, \boldsymbol{w}_c) = \gamma_s \tag{7b}$$
$$\|\boldsymbol{w}_c\|^2 + \|\boldsymbol{w}_s\|^2 \le P_{\max} \tag{7c}$$
$$\boldsymbol{w}_s, \boldsymbol{w}_c \in \mathcal{W}. \tag{7d}$$

Define $\boldsymbol{w} := [\boldsymbol{w}_s; \boldsymbol{w}_c] \in \mathbb{C}^{2N\times 1}$ such that $\boldsymbol{w}_s = \boldsymbol{T}_1 \boldsymbol{w}$ and $\boldsymbol{w}_c = \boldsymbol{T}_2 \boldsymbol{w}$ where $\boldsymbol{T}_1, \boldsymbol{T}_2$ are $N \times 2N$ selection matrices of

$\{0, 1\}$. Then, Problem (7) becomes

$$\max_{\boldsymbol{w}} \frac{\boldsymbol{w}^H \boldsymbol{T}_2^H \boldsymbol{h}_c \boldsymbol{h}_c^H \boldsymbol{T}_2 \boldsymbol{w}}{\boldsymbol{w}^H \boldsymbol{T}_1^H \boldsymbol{h}_c \boldsymbol{h}_c^H \boldsymbol{T}_1 \boldsymbol{w} + \sigma_c^2} \tag{8a}$$
$$\text{s.t. } \boldsymbol{w}^H \boldsymbol{A} \boldsymbol{w} = \sigma_s^2 \gamma_s \tag{8b}$$
$$\boldsymbol{w}^H (\boldsymbol{T}_1^H \boldsymbol{T}_1 + \boldsymbol{T}_2^H \boldsymbol{T}_2) \boldsymbol{w} \leq P_{\max} \tag{8c}$$
$$\boldsymbol{T}_1 \boldsymbol{w}, \boldsymbol{T}_2 \boldsymbol{w} \in \mathcal{W} \tag{8d}$$

where we have

$$\begin{aligned}\boldsymbol{A} :=& \boldsymbol{T}_1^H \boldsymbol{H}_{s,t} \boldsymbol{T}_1 - \gamma_s (\boldsymbol{T}_1 + \boldsymbol{T}_2)^H \boldsymbol{H}_{s,c} (\boldsymbol{T}_1 + \boldsymbol{T}_2) \\ &- \gamma_s \boldsymbol{T}_2^H \boldsymbol{H}_{s,t} \boldsymbol{T}_2\end{aligned} \tag{9}$$

With the definition of $\boldsymbol{W} := \boldsymbol{w}\boldsymbol{w}^H$, Problem (8) becomes

$$\max_{\boldsymbol{W}} \frac{\text{Tr}(\boldsymbol{T}_2^H \boldsymbol{h}_c \boldsymbol{h}_c^H \boldsymbol{T}_2 \boldsymbol{W})}{\text{Tr}(\boldsymbol{T}_1^H \boldsymbol{h}_c \boldsymbol{h}_c^H \boldsymbol{T}_1 \boldsymbol{W}) + \sigma_c^2} \tag{10a}$$
$$\text{s.t. } \text{Tr}(\boldsymbol{A}\boldsymbol{W}) = \sigma_s^2 \gamma_s \tag{10b}$$
$$\text{Tr}((\boldsymbol{T}_1^H \boldsymbol{T}_1 + \boldsymbol{T}_2^H \boldsymbol{T}_2)\boldsymbol{W}) \leq P_{\max} \tag{10c}$$
$$\text{Tr}(\boldsymbol{E}_1 \boldsymbol{W}) = \text{Tr}(\boldsymbol{E}_n \boldsymbol{W}), \forall n = 2, \ldots, N \tag{10d}$$
$$\text{Tr}(\boldsymbol{E}_{N+1} \boldsymbol{W}) = \text{Tr}(\boldsymbol{E}_{N+n} \boldsymbol{W}), \forall n = 2, \ldots, N \tag{10e}$$
$$\text{rank}(\boldsymbol{W}) = 1, \tag{10f}$$

which is non-convex even when the rank-one constraint $\text{rank}(\boldsymbol{W}) = 1$ is dropped, because the objective function is with a fractional structure and thus non-concave. To deal with the fractional objective function, we introduce an extra variable $\mu > 0$ such that the denominator can be removed, i.e.,

$$\mu(\text{Tr}(\boldsymbol{T}_1^H \boldsymbol{h}_c \boldsymbol{h}_c^H \boldsymbol{T}_1 \boldsymbol{W}) + \sigma_c^2) = 1 \tag{11}$$
$$\iff \text{Tr}(\boldsymbol{T}_1^H \boldsymbol{h}_c \boldsymbol{h}_c^H \boldsymbol{T}_1 \boldsymbol{X}) + \sigma_c^2 \mu = 1 \tag{12}$$

where $\boldsymbol{X} := \mu \boldsymbol{W}$ is a new semi-definite matrix variable. Then, based on the variable transfer $\boldsymbol{W} = \boldsymbol{X}/\mu$ and (11), the optimization of $\boldsymbol{W}$ in Problem (10) becomes an equivalent optimization problem with respect to $\{\boldsymbol{X}, \mu\}$, i.e.,

$$\max_{\boldsymbol{X} \succcurlyeq \boldsymbol{0}, \mu > 0} \text{Tr}(\boldsymbol{T}_2^H \boldsymbol{h}_c \boldsymbol{h}_c^H \boldsymbol{T}_2 \boldsymbol{X}) \tag{13a}$$
$$\text{s.t. } \text{Tr}(\boldsymbol{A}\boldsymbol{X}) = \sigma_s^2 \gamma_s \mu \tag{13b}$$
$$\text{Tr}((\boldsymbol{T}_1^H \boldsymbol{T}_1 + \boldsymbol{T}_2^H \boldsymbol{T}_2)\boldsymbol{X}) \leq \mu P_{\max} \tag{13c}$$
$$\text{Tr}(\boldsymbol{E}_1 \boldsymbol{X}) = \text{Tr}(\boldsymbol{E}_n \boldsymbol{X}), \forall n = 2, \ldots, N \tag{13d}$$
$$\text{Tr}(\boldsymbol{E}_{N+1} \boldsymbol{X}) = \text{Tr}(\boldsymbol{E}_{N+n} \boldsymbol{X}), \forall n = 2, \ldots, N \tag{13e}$$
$$\text{rank}(\boldsymbol{X}) = 1. \tag{13f}$$

If without the rank-one constraint, Problem (13) becomes a standard convex optimization problem of $\{\boldsymbol{X}, \mu\}$. Thus, a conventional way to deal with the non-convex rank-one constraint is semidefinite relaxation (SDR) based method - solve the completely relaxed optimization without the rank-one constraint firstly and then reconstruct the rank-one solution using the principal eigenvector or randomization [15]. Therefore, if $\boldsymbol{W}^\star$ is rank-one, the principal eigenvector of $\boldsymbol{W}^\star$ will be a tight optimal solution to Problem (13). However, $\boldsymbol{W}^\star$ usually has the rank of more than one, and thus it is inaccurate or even infeasible to use the principal eigenvector or randomization to approximate $\boldsymbol{w}$.

Driven by this issue, we propose a novel SROCR-based algorithm to attain a locally optimal rank-one solution. The basic framework of the SROCR method was proposed in [16]. We introduce a variable $\rho^{(i)} \in [0, 1]$ to *softly* relax the hard rank-one constraint. At the point $\boldsymbol{Z}$, Problem (13) becomes

$$\max_{\boldsymbol{X} \succcurlyeq \boldsymbol{0}, \mu > 0} \text{Tr}(\boldsymbol{T}_2^H \boldsymbol{h}_c \boldsymbol{h}_c^H \boldsymbol{T}_2 \boldsymbol{X}) \tag{14a}$$
$$\text{s.t. } \boldsymbol{X}, \mu \in \text{(13b)}, \text{(13c)}, \text{(13d)}, \text{(13e)} \tag{14b}$$
$$\boldsymbol{u}_{\max}(\boldsymbol{Z})^H \boldsymbol{X} \boldsymbol{u}_{\max}(\boldsymbol{Z}) \geq \rho^{(i)} \text{Tr}(\boldsymbol{X}), \tag{14c}$$

where $\boldsymbol{u}_{\max}(\boldsymbol{Z})$ denotes the largest eigenvector of $\boldsymbol{Z}$ associate with the largest eigenvalue $\lambda_{\max}(\boldsymbol{Z})$. We have

$$\boldsymbol{u}_{\max}(\boldsymbol{Z})^H \boldsymbol{X} \boldsymbol{u}_{\max}(\boldsymbol{Z}) \overset{(a)}{\leq} \lambda_{\max}(\boldsymbol{X}) \overset{(b)}{\leq} \text{Tr}(\boldsymbol{X}), \tag{15}$$

where the equality (a), and equality (b) hold only when $\boldsymbol{X} = \boldsymbol{Z}$, and $\text{rank}(\boldsymbol{X}) = 1$, respectively. Therefore, the equivalent rank-one constraint constraint $\lambda_{\max}(\boldsymbol{X}) = \text{Tr}(\boldsymbol{X})$ can be relaxed gradually as (14c), where the sequential increase of $\rho^{(i)}$ will scale the ratio of the largest eigenvalue to the trace of the solution $\boldsymbol{X}$ until $\rho^{(i)} = 1$ so that $\boldsymbol{X}$ becomes a rank-one solution to Problem (13), because (14c) implies $\lambda_{\max}(\boldsymbol{X}) / \text{Tr}(\boldsymbol{X}) \geq \rho^{(i)}$. The SROCR-based algorithm is described in Algorithm 1.

Algorithm 1 SROCR-based Algorithm for Problem (13)

Initialization: $i = 0$.
Solve Problem (14) w/o rank-one constraint and obtain $\boldsymbol{X}^{(0)}$.
Define an initial step size

$$\delta^{(0)} \in (0, 1 - \lambda_{\max}(\boldsymbol{X}^{(0)}) / \text{Tr}(\boldsymbol{X}^{(0)})]. \tag{16}$$

repeat
  Given $\{\rho^{(i)}, \boldsymbol{X}^{(i)}\}$, solve the convex problem (14);
  if *Problem* (14) *is solvable* **then**
    Obtain the optimal solution $\boldsymbol{X}^{(i+1)}$ to Problem (14);

$$\delta^{(i+1)} \leftarrow \delta^{(0)}; \tag{17}$$

  else

$$\delta^{(i+1)} \leftarrow \delta^{(i)}/2. \quad \text{\% reduce the step size} \tag{18}$$

$$\rho^{(i+1)} \leftarrow \min\left(1, \frac{\lambda_{\max}(\boldsymbol{X}^{(i+1)})}{\text{Tr}(\boldsymbol{X}^{(i+1)})} + \delta^{(i+1)}\right). \tag{19}$$

  $i \leftarrow i + 1$.
until $\rho^{(i-1)} \geq 0.99$ *& convergence of the objective function*;

To make $\boldsymbol{X}^{(i)}$ more likely to be feasible to Problem (14) in the next iteration, in general the step size $\delta^{(i)}$ should be small. Finally, Algorithm 1 converges to a locally optimal rank-one solution to Problem (13) [16]. Based on the convergent rank-one solution $\boldsymbol{X}^{(i)}$, we can construct the analog beamforming vectors for Problem (7) as follows

$$\boldsymbol{w}_s = \boldsymbol{T}_1 \sqrt{\lambda_{\max}(\boldsymbol{X}^{(i)}/\mu^{(i)})} \boldsymbol{u}_{\max}(\boldsymbol{X}^{(i)}/\mu^{(i)}) \tag{20}$$
$$\boldsymbol{w}_c = \boldsymbol{T}_2 \sqrt{\lambda_{\max}(\boldsymbol{X}^{(i)}/\mu^{(i)})} \boldsymbol{u}_{\max}(\boldsymbol{X}^{(i)}/\mu^{(i)}). \tag{21}$$

IV. Numerical Illustration

We simulate the MIMO radar channel as shown in Fig.2, where 10 clutter scatters are randomly distributed within the angular range $[0, 180^o]$, the random distances in $[20, 300]$ meter, and random radar cross section (RCS) in $[0, 3]$ square meters. The radar observing target is located with the range of 150 meter, the angle of $\theta_t = 90^o$, and the RCS of 2 square meters. The single communication user is located with the range of 150 meter and the angle of 50^o.

We firstly calculate the maximum sensing SINR value $\overline{\text{SINR}}_s$, which can be obtained by maximizing the single sensing SINR (without communication constraint). In the simulation, when the radar sensing SINR requirement $\gamma_s = \eta \times \overline{\text{SINR}}_s$ increases gradually with the ratio $\eta : 0.1 \rightarrow 0.95$, we observe that the optimal solutions $\boldsymbol{X}^{(0)}$ to Problem (13) w/o rank-one constraint using the conventional SDR method usually have high rank. That is, the ratio of the largest eigenvalue to its trace $\lambda_{\max}(\boldsymbol{X}^{(0)})/\operatorname{Tr}(\boldsymbol{X}^{(0)})$ is smaller than one in Fig. (3). Therefore, this motivates the development of the SROCR-based algorithm. Fig. 4 shows the joint power allocation for radar sensing and communication, where more power is allocated to sensing as the sensing SINR requirement increases gradually.

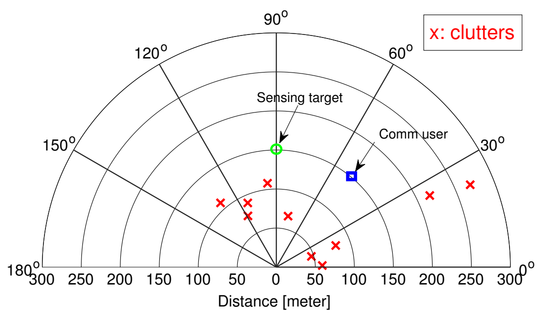

Fig. 2: Simulation scenario

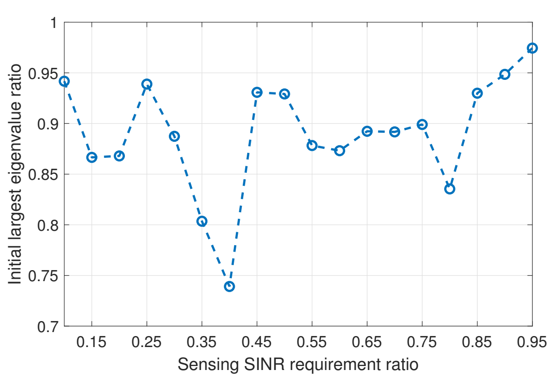

Fig. 3: Initial ratio $\lambda_{\max}(\boldsymbol{X}^{(0)})/\operatorname{Tr}(\boldsymbol{X}^{(0)})$

The achievable boundary of the ISAC SINR region is illustrated in Fig. 5, which is formed by solving a series operating point corresponding to $\gamma_s \in [0.1 : 0.95] \times \overline{\text{SINR}}_s$. The "proposed" boundary is achieved by our proposed SROCR-based algorithm, which serves as a locally Pareto optimal boundary. The proposed boundary is compared with two baselines: "SDR w/o normalization": By the SDR-based method ignoring the rank-one constraint, the obtained solution $\boldsymbol{X}^{(0)}$ is usually not rank-one as shown in Fig.3. Set $\boldsymbol{w} = \sqrt{\lambda_{\max}(\boldsymbol{X}^{(0)})}\boldsymbol{u}_{\max}(\boldsymbol{X}^{(0)})$ (not necessary constant-modulus); "SDR w/ normalization": Normalize element-wisely $\boldsymbol{w} = \sqrt{\lambda_{\max}(\boldsymbol{X}^{(0)})}\boldsymbol{u}_{\max}(\boldsymbol{X}^{(0)})$. The maximum sensing SINR $\overline{\text{SINR}}_s$ and the maximum communication SINR can be calculated for the single-function scenario - sensing only and communication only, respectively. In the comparison, we can observe that the proposed boundary outperforms the baselines.

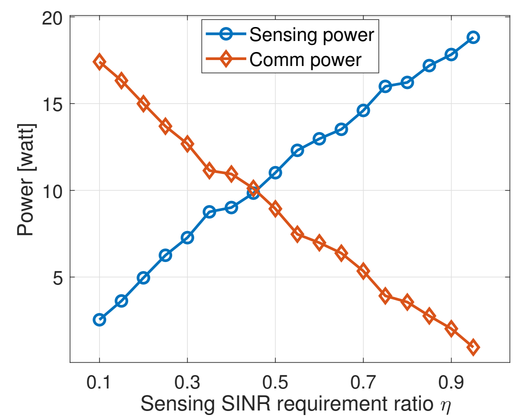

Fig. 4: Radar sensing power vs. Communication power [Watt]

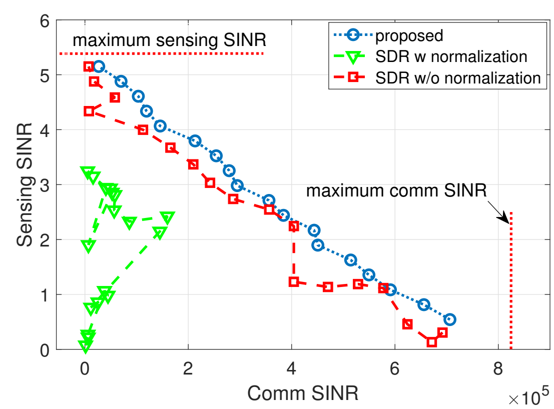

Fig. 5: Achievable boundary illustration and comparison

V. Conclusions

In this work, we formulate an optimization problem - maximize the communication SINR while the sensing SINR is fixed in order to determine a Pareto bound point of the ISAC SINR region. This is for the first time to study this type problem for the integrated MIMO radar and communication. We propose an SRCOR-based algorithm to attain locally optimal solutions, leading to a locally Pareto optimal inner boundary.

REFERENCES

[1] Aboulnasr Hassanien, Moeness G. Amin, Yimin D. Zhang, and Fauzia Ahmad, "Signaling strategies for dual-function radar communications: An overview," *IEEE Aerospace and Electronic Systems Magazine*, vol. 31, no. 10, pp. 36–45, 2016.

[2] A. R. Chiriyath, B. Paul, and D. W. Bliss, "Radar-communications convergence: Coexistence, cooperation, and co-design," *IEEE Transactions on Cognitive Communications and Networking*, vol. 3, no. 1, pp. 1–12, 2017.

[3] Bryan Paul, Alex R. Chiriyath, and Daniel W. Bliss, "Survey of RF communications and sensing convergence research," *IEEE Access*, vol. 5, pp. 252–270, 2017.

[4] Fan Liu, Christos Masouros, Athina P. Petropulu, Hugh Griffiths, and Lajos Hanzo, "Joint radar and communication design: Applications, state-of-the-art, and the road ahead," *IEEE Transactions on Communications*, vol. 68, no. 6, pp. 3834–3862, 2020.

[5] Thorsten Wild, Volker Braun, and Harish Viswanathan, "Joint design of communication and sensing for beyond 5G and 6G systems," *IEEE Access*, vol. 9, pp. 30845–30857, 2021.

[6] J. Andrew Zhang, Lushanur Rahman, Kai Wu, Xiaojing Huang, Y. Jay Guo, Shanzhi Chen, and Jinhong Yuan, "Enabling joint communication and radar sensing in mobile networks - A survey," *IEEE Communications Surveys & Tutorials*, 2021.

[7] An Liu, Zhe Huang, Min Li, Yubo Wan, Wenrui Li, Tony Xiao Han, Chenchen Liu, Rui Du, Danny Kai Pin Tan, Jianmin Lu, Yuan Shen, Fabiola Colone, and Kevin Chetty, "A survey on fundamental limits of integrated sensing and communication," *IEEE Communications Surveys & Tutorials*, pp. 1–1, 2022.

[8] Zhiqiang Xiao and Yong Zeng, "An overview on integrated localization and communication towards 6G," *Science China Information Sciences*, 2021.

[9] Pan Cao, "Cellular base station imaging for UAV detection," *IEEE Access*, vol. 10, pp. 24843–24851, 2022.

[10] H. J. M. Peters, "Game theory, mathematical programming and operations research," in *Axiomatic Bargaining Game Theory*. 1992, vol. 9, p. 14, Kluwer Academic Publis.

[11] Eduard A. Jorswieck, Erik G. Larsson, and Danyo Danev, "Complete characterization of the Pareto boundary for the miso interference channel," *IEEE Transactions on Signal Processing*, vol. 56, no. 10, pp. 5292–5296, 2008.

[12] Pan Cao, Eduard A. Jorswieck, and Shuying Shi, "Pareto boundary of the rate region for single-stream mimo interference channels: Linear transceiver design," *IEEE Transactions on Signal Processing*, vol. 61, no. 20, pp. 4907–4922, 2013.

[13] Rami Mochaourab, Pan Cao, and Eduard Jorswieck, "Alternating rate profile optimization in single stream MIMO interference channels," *IEEE Signal Processing Letters*, vol. 21, no. 2, pp. 221–224, 2014.

[14] Li Chen, Fan Liu, Weidong Wang, and Christos Masouros, "Joint radar-communication transmission: A generalized pareto optimization framework," *IEEE Transactions on Signal Processing*, vol. 69, pp. 2752–2765, 2021.

[15] Zhi-quan Luo, Wing-kin Ma, Anthony Man-cho So, Yinyu Ye, and Shuzhong Zhang, "Semidefinite relaxation of quadratic optimization problems," *IEEE Signal Processing Magazine*, vol. 27, no. 3, pp. 20–34, 2010.

[16] P. Cao, J. Thompson, and H. V. Poor, "A sequential rank-one constraint relaxation algorithms for rank-one constrainted problems," in *EUSIPCO*, Aug. 2017.